

Low-Energy High-Precision Experiments

Kanishk¹, Kirana K.K.²

¹Indian Institute of Science

²Indian Institute of Science

Abstract: In this paper, we will look at some Low-Energy Experiments specifically, experiment with Ultra-Cold Neutrons (UNC) and the Pion-Beta Decay and how their high precision measurements have yielded some essential results in the Standard model.

1. Introduction

Historically, most of the experiments done in physics fall under the category of low-energy high-precision experiments and they have an instrumental role in the development of physics. In modern terms, low energy experiment refers to experiments that operate on an energy scale far below the ones used in the Large Hadron Collider (LHC). High-precision measurements of such experiments often yield deviation from the accepted understanding of physics which motivates the need for modifications to the theory to account for the deviations.

2. Non-Newtonian Gravitational field in range $1\mu\text{m}$ to $10\mu\text{m}$

2.1. Quantum Physics is Gravitational Field

Classical physics is a great description of the world on a large scale. But problems start arising when we try to move to the scale of atoms. For scale, quantum mechanics become a better description of the world. The Fall Experiment of Galileo Galilei is no different. Quantum theory when applied to particles freely falling under gravity does not fall continuously. The discrete energy levels of quantum particles falling under gravity are used to study the small-scale effects of gravity and corrections to Newtonian gravity.

Ultra-cold neutrons (UCN) are used to study the effect of gravity because they are heavy, long-lived and neutral. The gravitational energy of these neutrons in the ground state is of the order of peV whereas, the electromagnetic energy is of the order of 10^{-16} peV.

2.2. Non-Newtonian Gravity below $10\mu\text{m}$

The Newtonian potential for gravity is given by the inverse square law. Assuming that the deviation from this is in the form of the Yukawa potential for masses m_1 and m_2 and distance r . The modified potential ($V(r)$) is given by:

$$V(r) = -G \frac{m_1 m_2}{r} (1 + \alpha \cdot e^{-r/\lambda})$$

where G is the gravitational constant, λ is the Yukawa distance and α is the strength factor. Consider a neutron kept on top of a big mirror that reflects all neutrons falling on it (like an optical mirror reflects light). The neutron experiences force from the mirror as well as the rest of the earth. The gravitational force on neutrons from the earth leads to a free fall acceleration (g_E)

$$g_E = \frac{Gm_E}{R_E^2} = \frac{4}{3}\pi G\rho R_E$$

When the neutron is very close to the mirror the Yukawa-like interactions will modify this free-fall acceleration by g_m . Since the mirror is quite big we can assume it to be an infinite plane with mass density ρ exerting gravitational force on the neutrons above it.

$$V_m(z, \lambda) = 2\pi\rho\alpha\lambda^2 m_n G e^{-z/\lambda} \quad g_m = 2\pi\rho\alpha\lambda G e^{-z/\lambda}$$

This gives us the ratio

$$\frac{g_m(z, \lambda)}{g_E} = \frac{3}{2}\alpha \cdot \frac{\lambda}{R_E} \cdot e^{-z/\lambda}$$

Putting an upper limit on the correction to the free-fall acceleration (g_m) will give us a constraint on the value of α and λ

2.3. Experiment at Institut Laue-Langevin

2.3.1. Making UCN

Neutrons used in this experiment are taken from research reactors. The neutrons are produced at a temperature of 10^{10} K and an average energy of 2 MeV. These are thermalized in a tank of heavy water and brought to a temperature of 300 K. Then they are again thermalized in a second moderator (containing cold liquid deuterium) with a temperature of 25 K. The neutron follows the Maxwell energy distribution. The cold neutron velocity spectrum is obtained by passing the neutrons through a curved Nickel guide that absorbs a neutron above a threshold energy. These neutrons then collide with the rotating nickel blades of a turbine. Neutrons with 1 mK temperature exit the blade. These are still cooled by passing them through a collimator absorber system that reduces their energy to peV scale.

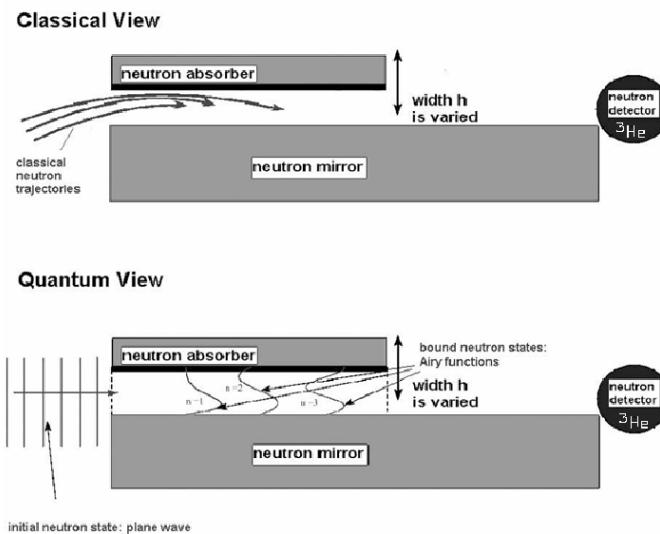
	fission neutrons	thermal neutrons	cold neutrons	ultracold neutrons	this experiment
Energy	2 MeV	25 meV	3 meV	100 neV	1.4 peV
Temperature	10^{10} K	300 K	40 K	1 mK	-
Velocity	10^7 m/s	2200 m/s	800 m/s	5 m/s	$v_{\perp} \sim 2$ cm/s

2.3.2. The setup

The experimental setup consists of a neutron mirror (/reflector), a neutron absorber, and a neutron detector. The neutron mirror uses the fact that strong forces from the nuclei in the mirror repel the neutron if its energy is lower than the fermi potential. When the roughness of the mirror is smaller than the de Broglie wavelength of the neutron then the neutron does not scatter after reflection. The mirror used in this experiment is a $10\text{cm} \times 10\text{cm} \times 3\text{cm}$ made up of optical glass kept mounted on an antivibration table. The fermi potential of glass is 100 neV. The roughness of the mirror is found using X-ray and it was found to be $\sigma = 2.2 \pm 0.2$ nm. The de Broglie wavelength of the neutron is in the range 40 nm to 100 nm.

The neutron absorber is made up of a rough glass plate coated with Gd-Ti-Zr alloy using magnetron evaporation. The absorbing layer is 200 nm thick. The roughness of the absorber was calculated using an atomic force microscope and it was found to be $\sigma = 0.75$ μm . The absorber removes the neutron both by the process of absorption and scattering. The height of the absorber is adjustable and it is used to remove high-energy neutrons. The absorber was found to have an efficiency of 93%.

This experiment uses a ^3He counter for the detection of neutrons. The setup is placed in a way such that the classical trajectory of the neutron hits the mirror twice.



2.3.3. Quantum Mechanical Description

The system can be described very well using the Schrodinger equation. Ignoring the Yukawa potential term, the system is under a potential given by $V(z) = mgz$ for $z > 0$ with $g = -G \frac{m_E}{R_E}$.

$$\left(-\frac{\hbar^2}{2m}\nabla^2 + V(z)\right)\psi = E\psi$$

The boundary condition on the wavefunction (ψ) should be that $\psi(z) = 0$ at $z = 0$. This gives us the wave function to be an Airy function.

$$\psi_n(z) = Ai\left(\frac{z}{z_0} - \frac{z_n}{z_0}\right)$$

$$z_n = z_0\left(\frac{3\pi}{2}\left(n - \frac{1}{4}\right)\right)^{2/3}$$

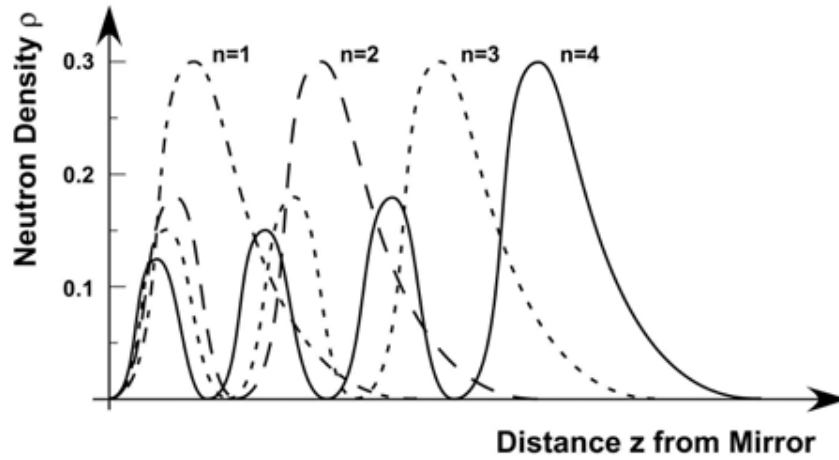
$$z_0 = \left(\frac{\hbar^2}{2m^2g}\right)^{1/3}$$

$$E_n = mgz_n$$

where z_n is the classical turning point of the n^{th} energy state with energy E_n .

Table 1. Neutron Energy level under potential $V = mgz$

n	z_n (in μm)	E_n (in peV)
1	13.7	1.44
2	24.1	2.53
3	32.5	3.42

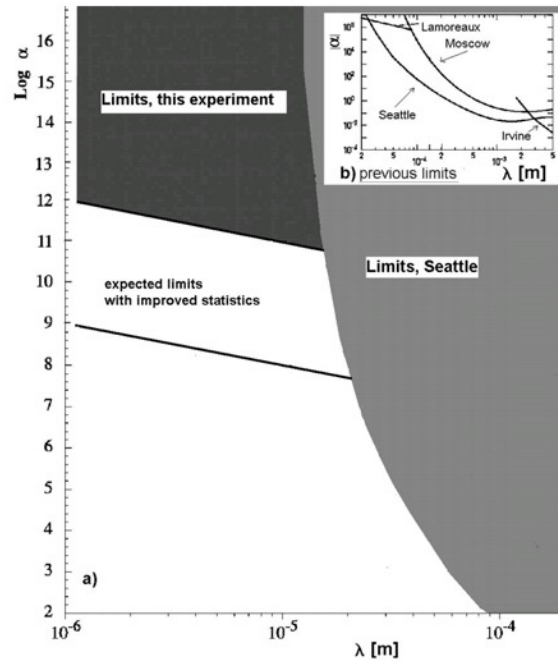
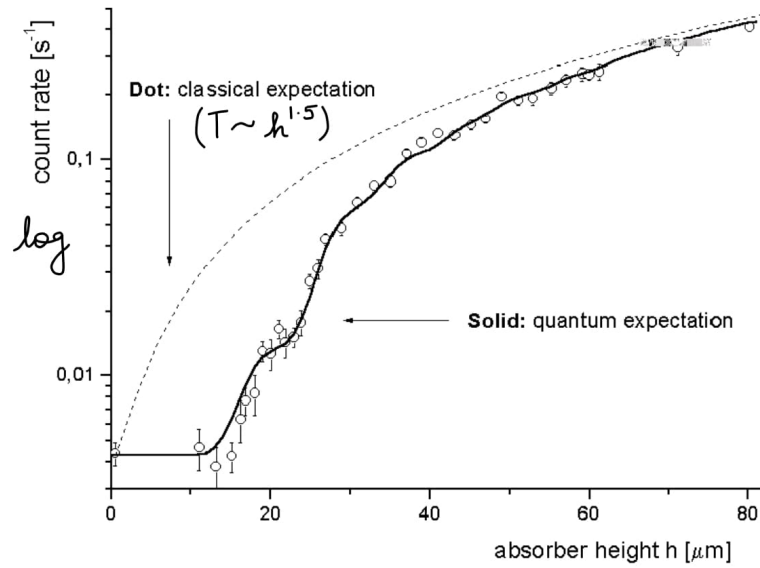


2.3.4. Results

Classically the number of neutrons reaching the detector per second (T) is proportional to the phase space volume allowed by the neutron absorber. Increasing the height of the absorber increases the phase space of the neutron. It is governed by the power law $T \sim h^{1.5}$. We find the transmission rate (T) using the ^3He absorber and plot it against the absorber height (h).

The dotted line is the classical phase space prediction. The solid lines are quantum expectation and the dots are the measured data points. At large absorber height, the quantum prediction approaches the classical predictions. T increases as a step function at small h and no neutron are detected below absorber height of $15\mu\text{m}$. The deviation of the data points from the quantum prediction is used to detect any deviation in the value of g at the small scale.

The experiment was successful in putting new constraints on the ratio $\frac{g_m}{g_E}$. They exclude any gravity-like interaction at $1\mu\text{m}$ range with strength more than 10^{12} . At $\lambda = 10\mu\text{m}$ the upper limit on α is found to be 10^{11} .



Limits for non-Newtonian gravity: Strength $|\alpha|$ vs. Yukawa length scale λ
a) Experiments with neutrons place limits for $|\alpha|$ in the range $1 \mu\text{m} < \lambda < 10 \mu\text{m}$.
b) Constraints from previous experiments

2.3.5. Discussion

The experiments done at ILL, Grenoble are a perfect example of low-energy high-precision experiments. In this experiment, gravitational bound states have been observed for the first time and they are in good agreement with the quantum mechanical predictions at the scale of $1 \mu\text{m}$. Further refinement in the experimental results can be obtained by lowering the error bar for the data points by increasing the detector efficiency and better modelling of the absorber used in this experiment.

3. Precision Studies of Pions: Scattering, Decay, and the Standard Model

3.1. Theoretical Foundations of Pion Physics

In the early development of nuclear physics, the nature of the force-binding protons and neutrons (collectively called nucleons) was poorly understood. To explain the short-range nature of these interactions, **Hideki Yukawa** proposed the existence of massive spin-0 bosons, now known as *pions*. These particles were later experimentally discovered and are known to exist in three charge states: π^+ , π^0 , and π^- , with masses slightly above $135 \text{ MeV}/c^2$, significantly lighter than nucleons, which are around $939 \text{ MeV}/c^2$.

In modern theoretical physics, pions are understood as low-energy effective degrees of freedom that emerge when the fundamental constituents—quarks and gluons—become confined. At such low energies, the physics is governed not by free quarks and gluons but by composite particles: *baryons* (three-quark systems) and *mesons* (quark-antiquark pairs). Pions are particularly light among hadrons due to a phenomenon called *spontaneous symmetry breaking* of a global symmetry in the framework of quantum chromodynamics (QCD).

An important conceptual development contributing to our understanding of pions is the idea of *isospin symmetry*, introduced by W. Heisenberg. He proposed that protons and neutrons behave like two states of a single particle under the strong interaction. This symmetry is approximately valid because the up (u) and down (d) quarks have nearly equal masses. The next heavier quark, the *strange* (s) quark, contributes to the formation of heavier mesons known as *kaons*. Together with pions and the η meson, kaons form the *pseudo-scalar octet*, reflecting the underlying flavour symmetry of QCD.

This octet structure arises due to the breaking of the approximate $SU(3)_L \times SU(3)_R$ chiral symmetry to $SU(3)$, a process governed by the *Nambu-Goldstone mechanism*. The resulting pseudo-Goldstone bosons are the light mesons, including pions and kaons, whose relatively low masses are explained by this spontaneous symmetry breaking.

Because pions are the lightest strongly interacting particles, they serve as sensitive probes for testing predictions of the *Standard Model* (SM) in the low-energy regime. As bound states of light quark-antiquark pairs (u and d), pions provide valuable insight into the *non-perturbative* aspects of QCD, where traditional perturbation theory fails. Their interactions form the foundation of *chiral perturbation theory* (ChPT), an effective field theory that systematically describes low-energy hadron dynamics.

3.2. Neutral Pion Lifetime

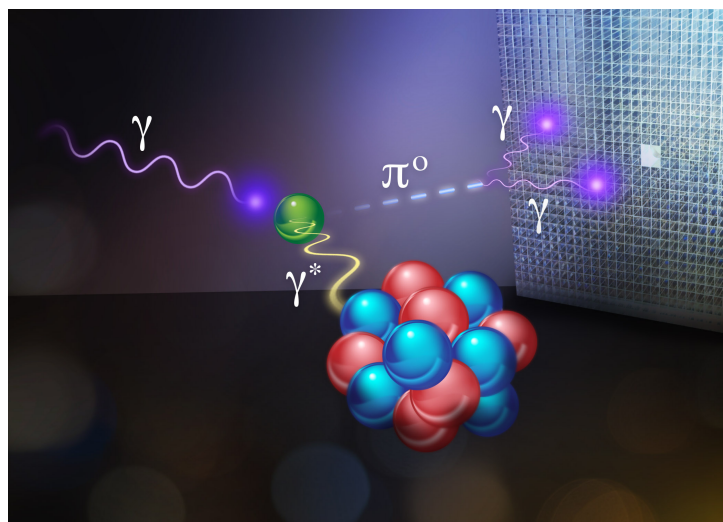


Fig. 1. Primakoff Effect

A particularly significant phenomenon involving pions is the decay of the neutral pion (π^0) into two photons:

$$\pi^0 \rightarrow \gamma\gamma$$

This decay is governed by the *chiral anomaly*, a quantum mechanical effect that breaks the classical conservation of the axial-vector current. Remarkably, the decay width is almost entirely determined by the *charged pion decay constant* (F_π), along with fundamental constants such as the fine-structure constant (α) and Planck's constant (\hbar). As a result, the measurement of the π^0 lifetime offers a clean and precise test of QCD and anomaly-related physics.

The *Primakoff effect*, named after Henry Primakoff, refers to the production of neutral pseudoscalar mesons, such as the π^0 , via the interaction of high-energy photons with atomic nuclei. This process is effectively the reverse of the decay of a neutral pion into two photons ($\pi^0 \rightarrow \gamma\gamma$), and thus provides a method to experimentally measure the pion's decay width and lifetime with high precision.

Importantly, this effect is also relevant in astrophysical contexts, where it could contribute to the production of hypothetical particles such as the *axion*, via the conversion of axions to photons in strong electromagnetic fields.

In the laboratory, precision measurements of the π^0 lifetime have been made using the Primakoff process, particularly in the *PrimEx experiment* at Jefferson Lab (JLab). These results are in excellent agreement with theoretical predictions based on the *chiral anomaly*, which relates the decay width to fundamental constants and the pion decay constant (F_π). The theoretical prediction for the decay width is:

$$\Gamma(\pi^0 \rightarrow 2\gamma) = \left(\frac{M_{\pi^0} \alpha}{4\pi F_\pi} \right)^2 \approx 7.760 \text{ eV}$$

which corresponds to a lifetime of approximately:

$$\tau = \frac{1}{\Gamma} \approx 8.38 \times 10^{-17} \text{ s}$$

The PrimEx experiment reported the measured value:

$$\Gamma = 7.82 \pm 0.14_{\text{(stat.)}} \pm 0.17_{\text{(syst.)}} \text{ eV}$$

This result aligns with theoretical corrections accounting for *isospin violation*, such as π^0 - η mixing, and confirms the predictions of anomaly-driven pion decay.

According to the 2018 *Review of Particle Physics*, the currently accepted value for the π^0 lifetime is:

$$\tau = (8.52 \pm 0.18) \times 10^{-17} \text{ s}$$

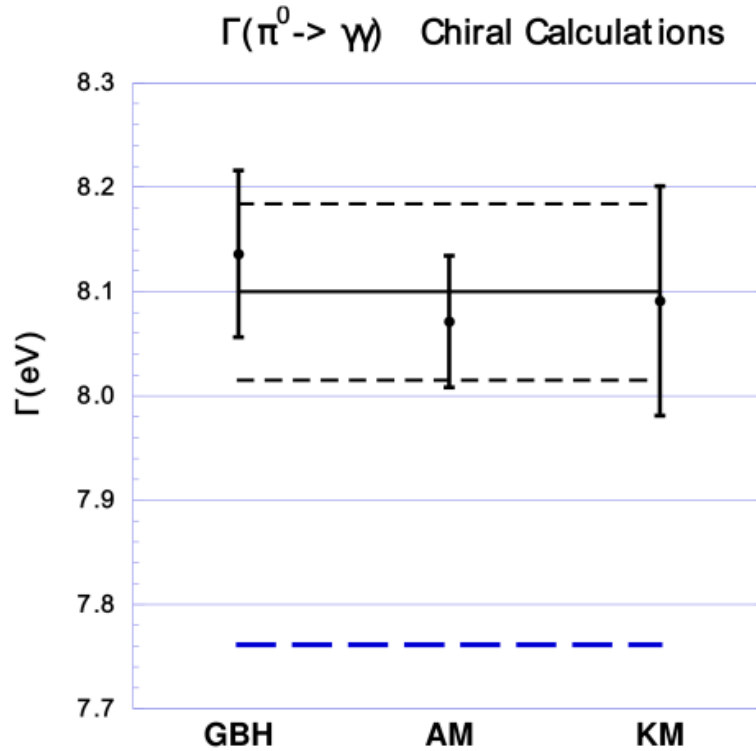


Fig. 2. Summary of chiral corrections. The large dashed line represents the anomaly prediction. The three points indicate theoretical predictions, while the upper solid line shows their average. The shaded band corresponds to a 1% uncertainty around the average.

3.3. Understanding Pion-Pion Scattering at Low Energies

In quantum mechanics, when a projectile scatters off a target, the key quantity that describes the interaction is the *scattering amplitude*. This amplitude is a complex function that depends on both the energy and momentum transfer between the particles, and it encodes the real and imaginary parts of the interaction strength.

To study scattering processes in detail—especially at low energies—the scattering amplitude is typically *decomposed into partial waves*, each associated with a definite angular momentum. These are denoted using spectroscopic notation such as S-, P-, D-, F-waves, and so on. At low energies, the contribution from higher angular momentum components is suppressed due to the centrifugal barrier, making the *lowest partial waves*, particularly the *S-wave* (with angular momentum $\ell = 0$), the most significant. Near the threshold of the scattering process, the real part of the amplitude can be expanded in powers of momentum, leading to the definition of key parameters such as the *scattering length* (e.g., a_0^0, a_0^2) and the *effective range*, which together quantify the strength and spatial extent of the interaction.

This formalism is especially important in the case of *pion-pion scattering*, a process of fundamental interest in hadronic physics. Pions form an *isospin triplet*, which means that the total isospin of a two-pion system can be 0, 1, or 2 depending on how the isospin components combine. This *isospin decomposition* allows one to express all physical scattering processes—such as $\pi^+\pi^+ \rightarrow \pi^+\pi^+$, $\pi^-\pi^+ \rightarrow \pi^-\pi^+$, and $\pi^+\pi^- \leftrightarrow \pi^0\pi^0$ —in terms of a small number of isospin amplitudes. These simplifications are particularly effective when small mass differences between charged and neutral pions are neglected.

Furthermore, the symmetry properties of pions, as bosons, introduce important constraints. According to *Bose statistics*, the overall wavefunction must be symmetric under particle exchange. As a result, *isospin-even amplitudes* (with $I = 0$ or $I = 2$) are associated only with even angular momentum states such as S- and D-waves, whereas *isospin-odd amplitudes* (with $I = 1$) must have odd angular momentum, such as P- or F-waves.

Historically, pion-pion scattering attracted significant theoretical interest even before the development of QCD. A major milestone in this context was the prediction by *Steven Weinberg*, who used current algebra and soft-pion theorems to compute the isospin-zero S-wave scattering length $a_0^0 \approx 0.16$ at *leading order* in the low-energy expansion. This prediction was later refined by *Gasser and Leutwyler*, who employed the techniques of *chiral perturbation theory* (ChPT) to calculate corrections at *next-to-leading order*, yielding $a_0^0 \approx 0.20 \pm 0.01$. Subsequent work including *higher-order corrections* confirmed the stability and accuracy of this result, demonstrating the power of ChPT in describing low-energy hadron dynamics with great precision.

In contrast, alternative theoretical approaches that are not as tightly constrained—such as certain phenomenological models or non-chiral frameworks—tend to predict *larger values* for the scattering length a_0^0 . This discrepancy underscores the *predictive power and internal consistency* of ChPT when built upon fundamental symmetry principles and the framework of effective field theory. Pion-pion ($\pi\pi$) scattering has long been a focal point in theoretical physics due to its relative simplicity and the ability to apply deep theoretical principles. Its study provided fertile ground for developing and testing fundamental concepts such as *unitarity*, *analyticity*, and *crossing symmetry*, all of which are grounded in general field-theoretical properties like *causality*.

One of the most significant outcomes of early work on scattering theory was the development of *dispersion relations*, which express scattering amplitudes as complex functions of energy using tools from complex analysis (such as Cauchy's theorem). However, early dispersion relation approaches contained ambiguities due to unknown functions of the momentum transfer, limiting their predictive power.

In 1971, **S.M. Roy** resolved many of these issues by deriving what are now known as the *Roy equations*. These are a system of coupled integral equations that relate the real parts of scattering amplitudes to their imaginary parts, with the only required inputs being the S-wave scattering lengths and some known partial wave data. This formulation represented a major theoretical advance, simplifying and unifying the treatment of $\pi\pi$ scattering.

The Roy equation analysis gained renewed attention in experimental physics when combined with data from rare decays such as K_{l4} decays. Using around 30,000 events from the Geneva-Saclay experiment, physicists were able to extract the isospin-zero S-wave scattering length:

$$a_0^0 \approx 0.26 \pm 0.05$$

validating predictions from *chiral perturbation theory*. Despite this success, activity in this field paused for several decades until the resurgence brought on by effective field theory and modern experimental techniques.

3.4. Scattering Lengths from NA48 and DIRAC Experiments

The NA48 collaboration at CERN has played a significant role in the precision measurement of pion-pion scattering lengths, which are fundamental parameters characterizing low-energy strong interactions. These measurements were obtained through two complementary experimental approaches that involved the decay of charged kaons (K^\pm).

One important result came from the observation of a subtle quantum mechanical effect known as the *cusp* in the decay process $K^\pm \rightarrow \pi^\pm \pi^0 \pi^0$. This idea, originally proposed by Nicola Cabibbo, relies on analyzing the invariant mass distribution of the two neutral pions in the final state. In this decay, the neutral pion pair ($\pi^0 \pi^0$) can undergo final-state rescattering through the intermediate channel $\pi^+ \pi^- \rightarrow \pi^0 \pi^0$. This rescattering introduces a non-analytic feature—a sharp change in the slope—of the $\pi^0 \pi^0$ invariant mass spectrum precisely at the point where the invariant mass equals twice the mass of the charged pion ($2m_{\pi^+}$). The emergence of the cusp arises from quantum interference between the direct decay channel and the rescattering process and is particularly sensitive to the difference between the S-wave scattering lengths a_{00} and a_{20} , which correspond to isospin 0 and 2 channels, respectively.

Using a remarkably large dataset of approximately 27 million $K^\pm \rightarrow \pi^\pm \pi^0 \pi^0$ events, the NA48/2 collaboration was able to resolve this cusp feature with high precision. From their analysis, they extracted the scattering length combination:

$$|a_0^0 - a_2^0| = 0.264 \pm 0.015$$

which marked a significant improvement in the experimental determination of low-energy $\pi\pi$ scattering parameters.

In addition to the cusp analysis, the collaboration employed a second technique that focused on the rare semileptonic decay of the charged kaon: $K^\pm \rightarrow \pi^\pm \pi^\mp l^\pm \nu_l$, a process commonly referred to as K_{l4} decay. This decay provides a clean laboratory for observing pion-pion rescattering in the final state. Because the decay kinematics grant direct access to the phase shifts of the $\pi\pi$ system, it serves as a powerful probe of the S-wave interaction. Theoretical foundations for interpreting such decays were laid by classic works from Pais and Treiman, and later by Cabibbo and Maksymowicz.

Based on an analysis of 370,000 K_{l4} events, the NA48 collaboration determined the isospin-0 S-wave scattering length to be:

$$a_0^0 = 0.256 \pm 0.011$$

This measurement not only corroborates the predictions of chiral perturbation theory (ChPT) but also supports the findings from the cusp-based method, lending strong experimental consistency to the theoretical framework.

A similar analysis was conducted by the E865 experiment at Brookhaven National Laboratory (BNL), which also studied K_{l4} decays and analyzed approximately 400,000 events. Their reported value for the scattering length was:

$$a_0^0 = 0.216 \pm 0.015$$

Although slightly lower than the NA48 result, it remains broadly consistent within the experimental uncertainties.

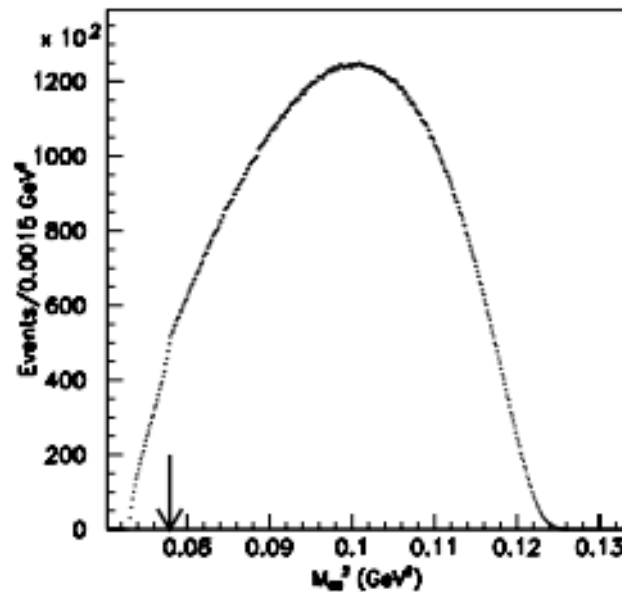


Fig. 3. Cusp Effect

All of these results—from both the cusp effect and K_{l4} decay analyses—are interpreted within the framework of the *Roy equations*, which relate scattering amplitudes through dispersion relations. By combining experimental phase shift data with low-energy theoretical constraints, the Roy equation analysis allows for the precise and reliable extraction of pion-pion scattering lengths.

An essential contribution to the precision study of low-energy quantum chromodynamics (QCD) comes from the DIRAC experiment (Di-Meson Relativistic Atom Complex), conducted at CERN. This experiment focuses on the production and lifetime measurement of a rare and exotic atomic system known as *pionium*.

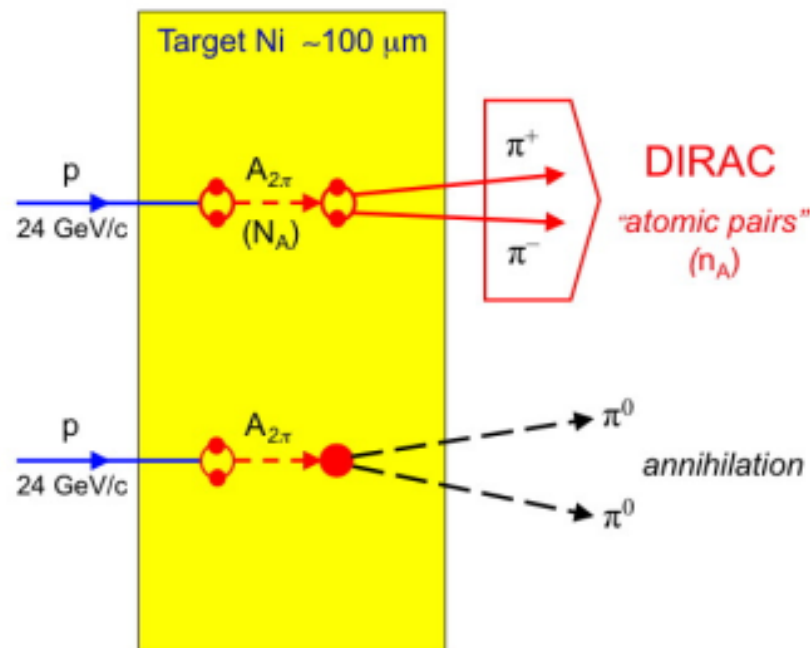


Fig. 4. DIRAC Experiment

Pionium is a short-lived, hydrogen-like bound state consisting of a positively charged pion (π^+) and a negatively charged pion (π^-). Although these mesons are strongly interacting particles, they can form a bound state via electromagnetic attraction, in a manner analogous to the way electrons and protons form hydrogen atoms. However, unlike hydrogen, pionium is highly unstable and decays primarily through the process:

$$\pi^+ \pi^- \rightarrow \pi^0 \pi^0$$

This decay occurs as a result of the strong interaction once the electromagnetic binding is disrupted.

The significance of pionium lies in the fact that its *lifetime is extremely sensitive* to the difference between two pion-pion scattering lengths:

$$|a_0^0 - a_0^2|$$

These quantities describe the strength of $\pi\pi$ interactions in the S-wave for isospin 0 and 2 channels, respectively. The difference between them is a key parameter in chiral perturbation theory (ChPT), offering a clean and precise test of low-energy QCD. This relationship was theoretically predicted over 50 years ago by S. Deser, M. L. Goldberger, K. Baumann, and W. E. Thirring, who showed that the pionium lifetime is directly related to $\pi\pi$ scattering parameters.

To carry out this investigation, the DIRAC collaboration at CERN developed advanced detectors and beamline technology to create and detect pionium atoms. These atoms are produced when high-energy proton collisions generate π^+ and π^- pairs, which subsequently slow down and form bound states via Coulomb attraction. Once formed, the atoms decay into neutral pion pairs ($\pi^0\pi^0$), and their lifetime—approximately 2 femtoseconds (2×10^{-15} s)—is determined by analyzing the timing and distribution of the decay products.

From a dataset containing around 6,600 ponium atoms, the DIRAC collaboration extracted the value:

$$|a_0^0 - a_0^2| = 0.264^{+0.033}_{-0.020}$$

This result is in remarkable agreement with the measurement obtained via the cusp effect observed in the NA48 experiment. The consistency between these two independent approaches confirms theoretical predictions derived from effective field theory and highlights the robustness of low-energy QCD in describing pion interactions.

3.5. Testing CKM Unitarity with Pion Beta Decay and the R_V Ratio

The Cabibbo–Kobayashi–Maskawa (CKM) matrix describes the mixing between quark flavors under the weak interaction. As a unitary 3×3 matrix, it must satisfy:

$$V^\dagger V = V V^\dagger = I$$

This unitarity leads to constraints on the matrix elements. In particular, the first row must satisfy:

$$|V_{ud}|^2 + |V_{us}|^2 + |V_{ub}|^2 = 1$$

Neglecting the tiny $|V_{ub}|^2 \sim 2 \times 10^{-5}$, we obtain:

$$|V_{ud}|^2 + |V_{us}|^2 \approx 1$$

Testing this relation at high precision is one of the most sensitive probes of new physics beyond the Standard Model (SM).

Precise values of $|V_{ud}|$ are typically extracted from superallowed nuclear beta decays, while $|V_{us}|$ is determined from semileptonic kaon decays (K_{l3}). These decays are analyzed using effective field theories like Chiral Perturbation Theory (ChPT) and inputs from lattice QCD, particularly for hadronic form factors and decay constants.

3.6. Radiative Corrections and Form Factors

Semileptonic decays are sensitive to both short-distance electroweak and long-distance QED corrections. The decay amplitudes also depend on form factors, which encode the non-perturbative QCD effects between hadrons. For example, the $K \rightarrow \pi$ transition involves the vector form factor $f_+(q^2)$, typically evaluated at zero momentum transfer, $f_+(0)$.

Lattice QCD provides high-precision predictions for $f_+^K(0)$, with typical values in the range 0.968–0.970. These are crucial inputs for extracting CKM elements from decay rates.

4. Pion Beta Decay

Pion beta decay ($\pi^+ \rightarrow \pi^0 e^+ \nu(\gamma)$) is a rare but theoretically clean process governed solely by the vector part of the weak current. The decay width is given by:

$$\Gamma(\pi^+ \rightarrow \pi^0 e^+ \nu(\gamma)) = \frac{G_\mu^2 |V_{ud}|^2 m_{\pi^+}^5}{64\pi^3} f_+^2(0) (1 + \text{RC}_\pi) I_\pi$$

with radiative correction $\text{RC}_\pi = 0.0334(10)$ and phase space factor I_π computed using ChPT.

From the measured branching ratio and pion lifetime:

$$\text{BR} = 1.038(6) \times 10^{-8}, \quad \tau_\pi = 26.033(5) \text{ ns}$$

the decay rate is:

$$\Gamma = 0.3988(23) \text{ s}^{-1}$$

yielding an extracted value:

$$|V_{ud}| = 0.9739(29)$$

This value is consistent with CKM unitarity but limited by experimental uncertainty (0.6%).

4.1. Vector Current Ratio R_V

A clean test of $|V_{us}|/|V_{ud}|$ arises from the ratio:

$$R_V = \frac{\Gamma(K_L \rightarrow \pi^\pm e^\mp \nu(\gamma))}{\Gamma(\pi^+ \rightarrow \pi^0 e^+ \nu(\gamma))}$$

Both processes are governed by the vector current and share similar radiative corrections, which largely cancel in the ratio.

The kaon decay width is:

$$\Gamma(K_L \rightarrow \pi^\pm e^\mp \nu(\gamma)) = \frac{G_\mu^2 |V_{us}|^2 m_{K_L}^5}{192\pi^3} f_+^2(0) (1 + \text{RC}_K) I_K$$

Using:

$$\tau_{K_L} = 51.16(21) \text{ ns}, \quad \text{BR} = 0.4056(9)$$

we obtain the experimental value:

$$R_V^{\text{exp}} = (1.9884 \pm 0.0115 \pm 0.0093) \times 10^7$$

The theoretical prediction reads:

$$R_V^{\text{theory}} = \frac{1}{3} \left(\frac{m_{K^0}}{m_{\pi^+}} \right)^5 \left(\frac{f_+^K(0) |V_{us}|}{f_+^\pi(0) |V_{ud}|} \right)^2 \frac{I_K}{I_\pi} \cdot (1.000 \pm 0.002)$$

Matching theory and experiment gives:

$$\frac{f_+^K(0) |V_{us}|}{f_+^\pi(0) |V_{ud}|} = 0.22223(64) \quad (40)$$

Assuming $f_+^\pi(0) = 1$, this implies:

$$f_+^K(0) = 0.9607(38)$$

This result is in 2.2σ tension with lattice QCD estimates, typically around $f_+^K(0) = 0.970(2)$. Reversing the logic and using the lattice value instead yields:

$$\frac{V_{us}}{V_{ud}} = 0.22910(91)$$

This is also in tension with the unitarity-favored result from R_A .

4.2. Discussion

The discrepancy between lattice results and experimental extractions could be due to:

- A missing electromagnetic correction of approximately -0.01 in the lattice prediction of $f_+^K(0)$,
- Or the emergence of new physics not captured by the Standard Model.

Using the adjusted CKM ratio and enforcing unitarity gives:

$$|V_{ud}| = 0.97474(22)$$

which exceeds values from nuclear beta decay, further complicating the picture.

While averaging over all K_{l3} decay modes has reduced kaon-related uncertainties, the dominant error now arises from pion beta decay. A factor of 2–3 improvement in its measurement would halve the total uncertainty in R_V . Alongside better precision in R_A , this would allow a powerful test of CKM unitarity and potentially uncover deviations pointing to new physics.

5. References

References

1. H. Abele, S. Baebler and A. Westphal *Quantum States of Neutrons in the Gravitational Field and Limits for Non-Newtonian Interaction in the Range between 1 μm and 10 μm* , [arXiv:hep-ph/0301145 \[hep-ph\]](#) (2003).
2. B. Ananthanarayan and S. Ghosh, *Pion Interactions and the Standard Model at High Precision*, Centre for High Energy Physics, Indian Institute of Science, [arXiv:1901.11061 \[physics.hist-ph\]](#) (2018).
3. A. Czarnecki, W. J. Marciano, and A. Sirlin, *Pion beta decay and Cabibbo-Kobayashi-Maskawa unitarity*, [arXiv:1911.04685 \[hep-ph\]](#) (2020).
4. G. Lamanna, *Pion-pion scattering lengths from Ke4 and Cusp at NA48/2 experiment*, *Nucl. Phys. B (Proc. Suppl.)* **186** (2009) 322–325, [doi:10.1016/j.nuclphysbps.2008.12.058](#).